Analog computation of wavelet transform coefficients in real-time

Transactions Briefs

Analog Computation of Wavelet Transform Coefficients in Real-Time

Oscar Moreira-Tamayo and José Pineda de Gyvez

***Abstract*—This brief presents a time-domain approach for the implementation and continuous generation of wavelet transform coefficients for spectral analysis applications. The wavelet generation relies on amplitude modulation techniques. This approach offers two extra degrees of freedom through the appropriate use of the modulation index and the selected envelope signal. The added flexibility along with choice of frequencies allows to generate different time-frequency windows with equal resolution for all frequencies. A convolution (correlator) circuit that computes the wavelet transform and delivers the coefficient corresponding to each wavelet was designed to substantiate theoretical findings. Experimental results of a hardware prototype are presented.**

I. Introduction

Wavelet transforms can be used for signal processing or for signal analysis. In signal processing they are used to adapt or to transform the signal for some specific purposes such as filtering, compression, etc. While in spectral analysis they are utilized to extract information about the frequency contents of a signal. This is the main focus of this brief. Applications of spectral analysis include spectrogram computation for speech recognition, echo detection for radar applications, detection of spikes for machine failure diagnosis, screening of heart anomalies for medical diagnosis, etc. These applications have in common that they do not require reconstruction of the input signal. The requirements on each application vary from obtaining a representation of the signal's spectrum covering all frequencies on a given range (spectrogram), to just detecting the presence of some frequency components in a certain time. For the latter case the wavelet set is not required to be a complete set. An optimum solution for these problems provides the required accuracy with minimum computation time and hardware. The system described in this brief can be considered as a high quality frequency to voltage converter with adjustable time-frequency windows for best accuracy.

The main advantages of the system hereby proposed are the high speed and low cost of analog electronics. Time-frequency windows can be generated for signal analysis to provide the same resolution for different frequencies. As it will be seen, these time-frequency windows are computed simultaneously as the input signal is received providing an output with very small delay.

In this brief we operate with continuous-time signals and compute a discrete number of coefficients of the continuous wavelet transform (CWT) in both the time and frequency domains. The implementation is intended only for frequency to voltage transformations. CWT transform requires an infinite number of coefficients to be able to decompose and reconstruct a signal. It is practically impossible to implement the CWT in time-domain since the required number of coefficients is infinite.

Manuscript received November 3, 1994; revised November 13, 1995. This work was supported in part by CONACyT, the National Council of Science and Technology of Mexico. This paper was recommended by Associate Editor Y. Inouye.

The authors are with the Department of Electrical Engineering, Texas A&M University, College Station, TX 77843 USA.

Publisher Item Identifier S 1057-7122(97)00814-3.

A wavelet transform can be implemented in the frequency or in the time-domain. The first case involves the design of filters. Reported implementations consist of modulated filter banks [1], [2] and switched capacitor techniques [3]. The time-domain implementation involves the design of wavelet generators, multipliers, and integrators in order to perform the convolution of the signal with the wavelet.

II. Wavelet Generation Through Amplitude Modulation

For many applications, the most important parameters in spectral analysis are time localization and frequency resolution. These two parameters define the time-frequency window that is being produced. The selection of the wavelet and its size is determined by the time-frequency window specifications. Let us consider now Gabor wavelets which consist of complex exponentials limited by a time window [4]. The size of the time-frequency window can be defined as the product of its root mean squared (rms) time and frequency durations [4], [5] represented as D_t, and D_f, respectively,

$$D_t^2 = \frac{1}{E}\int_{-\infty}^{\infty} t^2 v^2(t)\,dt, \tag{1a}$$

$$D_f^2 = \frac{1}{2\pi E}\int_{-\infty}^{\infty} \Omega^2 |V(j\Omega)|^2\,d\Omega \tag{1b}$$

where $v(t)$ is the window function used to modulate the complex exponential, E is the window energy, i.e., $E = \int v^2(t)\,dt$, D_t is the rms time-domain duration and D_f is the frequency domain duration of $v(t)$. Throughout the course of this section $v(t)$ is assumed to be real. There is a tradeoff between time localization and frequency resolution. If a window in the time-domainomain is narrow, its frequency domain characteristic is broad and vice versa. The product $D_t D_f$ is fixed for a given wavelet and it cannot be arbitrarily small as stated by the uncertainty principle, i.e., $D_t D_f \geq 0.5$. Equality is reached only if the window $v(t)$ is Gaussian [4]. Sinusoidal wavelets are an approximation to this minimum window as it will be shown in the rest of this section.

Many practical applications involving spectral analysis require a continuous analysis of the signal. The corresponding wavelet transforms need to be computed repeatedly using a scaled and shifted version of the basic wavelet. In order to perform these operations a wavelet chain is proposed. A wavelet chain consists of a sequence of wavelets generated consecutively one after another. Fig. 1 shows a chain of Spline [4] wavelets. Each wavelet in the chain can be maintained equal or be adjusted to a specific size depending upon the application. For instance, in Fig. 1 the wavelets are being successively scaled. Chains of sinusoidal wavelets can easily be generated by modulating a complex exponential signal with a lower frequency sinusoidal signal, i.e., a sinusoidal wavelet is defined as

$$\psi_s(t) := \begin{cases} A_c e^{-j\omega_c t}[1 + m\,\cos(\omega_p t)], & \text{for } -\pi < \omega_p t < \pi, \\ & \omega_p < \omega_c \\ 0, & \text{elsewhere} \end{cases} \tag{2}$$

where A_c is a reference magnitude of the wavelet, ω_c is the frequency being analyzed (*analyzing frequency*), ω_p is the frequency of the envelop and m is the modulation index. The lower and upper bounds of this wavelet are given as $l_i = -\pi/\omega_p$ and $l_f = \pi/\omega_p$, respectively. One can conclude that the time duration

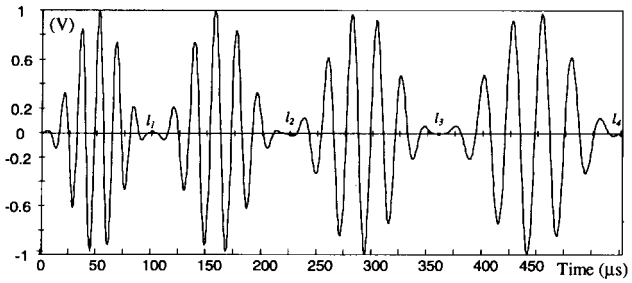

Fig. 1. Wavelet chain.

is $2\pi/\omega_p$. It can be seen from the limits imposed by (2), that the wavelet has a finite support. This wavelet is suitable for time-domain analog implementations since it is formed by sinusoidal signals which can be generated with simple circuits. Moreover, the shape of the envelope signal can be changed as well. Consider for instance a triangular signal (Barlett window [6]) which also can be easily implemented by integrating square signals. Obviously, the resulting wavelet is different from the one using sinusoidal envelopes. Now let us investigate the condition for these functions to be admissible wavelets. This condition is given by $\int \psi(x)\,dx = 0$. Strictly speaking, the condition on ψ should be $\int |\Psi(\omega)|^2 |\omega|^{-1}\,d\omega < \infty$, where Ψ is the Fourier transform of ψ; if $\psi(t)$ decays faster than $|t|^{-1}$ for $t \to \infty$, this condition is equivalent to the one above [7]. The wavelets in this paper meet this requirement since they have finite support. Thus

$$\begin{aligned}\int \psi(t)\,dt &= \frac{A_c e^{-j\pi n\omega_c t}}{\omega_c \pi n(\pi^2 n^2 - 1)}\,(-\sin(\pi n\omega_c t) \\ &\quad + j\{\pi^2 n^2[1+\cos(\omega_c t)] - 1\})|_{-\pi/\omega_p}^{\pi/\omega_p} \\ &= 2A_c \frac{(1-m)-1}{(n^2-1)\omega_p}\sin(n\pi) \qquad (3)\end{aligned}$$

where $n = \omega_c/\omega_p$. Notice that (3) is equal to zero if ω_c is an integer multiple of ω_p, i.e., n is an integer. Also notice that the function approaches zero if the constant n is big enough, i.e.,

$$\lim_{n\to\infty}\left[2A_c\frac{(1-m)-1}{(n^2-1)\omega_p}\sin(n\pi)\right] = 0. \qquad (4)$$

The last condition is commonly met in practical applications. The modulation index adds an extra degree of freedom as different time windows can be computed using the same expression by varying only m. For example, if the modulating index m is 1 or 23/27 we have wavelets based on the Hanning or Hamming window, respectively.

Now, let us analyze the size of the time frequency window for a sinusoidal wavelet based on the Hanning windows used in (2) with $A_c = 1$. Its rms duration is calculated as follows [8]:

$$\begin{aligned}D_t^2 &= \frac{1}{E}\int_{-\pi/\omega_p}^{\pi/\omega_p} t^2[1+\cos(\omega_p t)]^2\,dt \\ &= \frac{-15+2\pi^2}{6\omega_p^2}, \qquad (5)\end{aligned}$$

$$\begin{aligned}D_f^2 &= \frac{1}{2\pi E}\int_{-\infty}^{\infty}\omega^2\left|\frac{\omega_p^2}{\omega(\omega_p^2-\omega^2)}\sin\left(\frac{\omega\pi}{\omega_p}\right)\right|^2 d\omega \\ &= \frac{\omega_p^2}{3}. \qquad (6)\end{aligned}$$

Observe that $D_t D_f = 0.5131173$, only 2.62% larger than the smaller possible window (Gaussian). If we consider that the conventional duration of each wavelet is $\Delta_t = 2\pi/\omega_p$, then solving for ω_p and substituting into (5) we have $D_t = \sqrt{(2\pi^2 - 15/6}\,(\Delta t/2\pi) = 0.1414\Delta t$. This result implies that the rms duration of the signal is 0.1414 of the conventional duration. Considering again the wavelet chain we can see now that the time-frequency windows are not continuous since the rms duration is smaller that the conventional duration. This is illustrated in Fig. 2 in which a time discontinuity or gap in the transition between two consecutive wavelets of the chain is shown. If the application requires this gap to be filled it can be done by having delayed chains of wavelets.

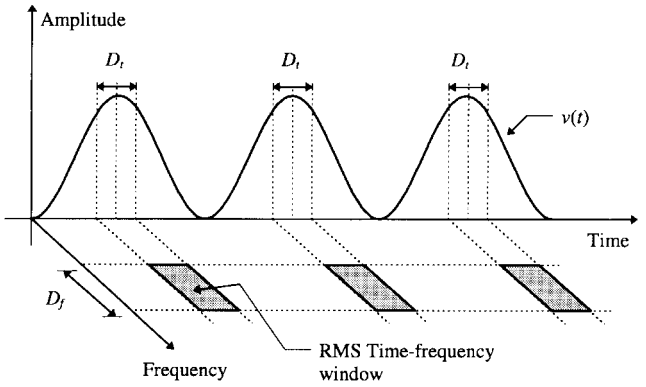

Fig. 2. Representation of time-frequency windows.

III. Implementation Procedure

The proposed approach consists of generating a chain of wavelets by multiplying two periodic functions. Each wavelet is then multiplied by the signal to be analyzed, $f(t)$, and integrated. The equation to be implemented in hardware is

$$\begin{aligned}(W_s f)(a,\,b) &= \frac{1}{\sqrt{a}}\int_{l_i}^{l_f} f(t) \\ &\quad \cdot\left[g\left(\frac{t-b}{a}\right)\cdot v\left(\frac{t-b}{a}\right)\right]^* dt \qquad (7)\end{aligned}$$

where $g(\cdot)$ is the analyzing signal, $v(\cdot)$ is a periodic window signal used as envelope in the modulation process, a is a variable that represents the frequency scaling of the wavelet, b is the time shift of the wavelet, and * denotes complex conjugation. The function in brackets in (7), $g(\cdot)v(\cdot)$, represents the actual wavelet. Recall that each wavelet is bounded by l_f and l_i which are given by the window signal. As an example, consider the case of Fig. 1 in which a set of valid limits are $l_i = l_1$ and $l_f = l_2$.

Let us consider the sinusoidal wavelets [see (2)]. We have that the analyzing signal $g(\cdot)$ specifies a complex sinusoidal consisting of two orthogonal functions expressed as follows:

$$g(t) = e^{-j\omega_c t} = \cos(\omega_c t) + j\,\sin(\omega_c t). \qquad (8)$$

The envelope function $v(\cdot)$ is formed by sinusoidal envelopes and can be generated with the signal

$$v(t) = \tfrac{1}{2}[1 + m\,\cos(\omega_p t)]. \qquad (9)$$

Then (7) turns into (noting that $\omega_p = \omega_c/n$)

$$\begin{aligned}(W_s f)(a,\,t_o) &= \frac{1}{\sqrt{a}}\int_{t_o - a\Delta t/2}^{t_o + a\Delta t/2} f(t)\,\cos\left(\frac{\omega_c t}{a}\right) \\ &\quad \cdot\frac{1}{2}\left[1 + m\,\cos\left(\frac{\omega_c t}{an}\right)\right]dt \\ &\quad + \frac{j}{\sqrt{a}}\int_{t_o - a\Delta t/2}^{t_o + a\Delta t/2} f(t)\,\sin\left(\frac{\omega_c t}{a}\right) \\ &\quad \cdot\frac{1}{2}\left[1 + m\,\cos\left(\frac{\omega_c t}{an}\right)\right]dt \qquad (10)\end{aligned}$$

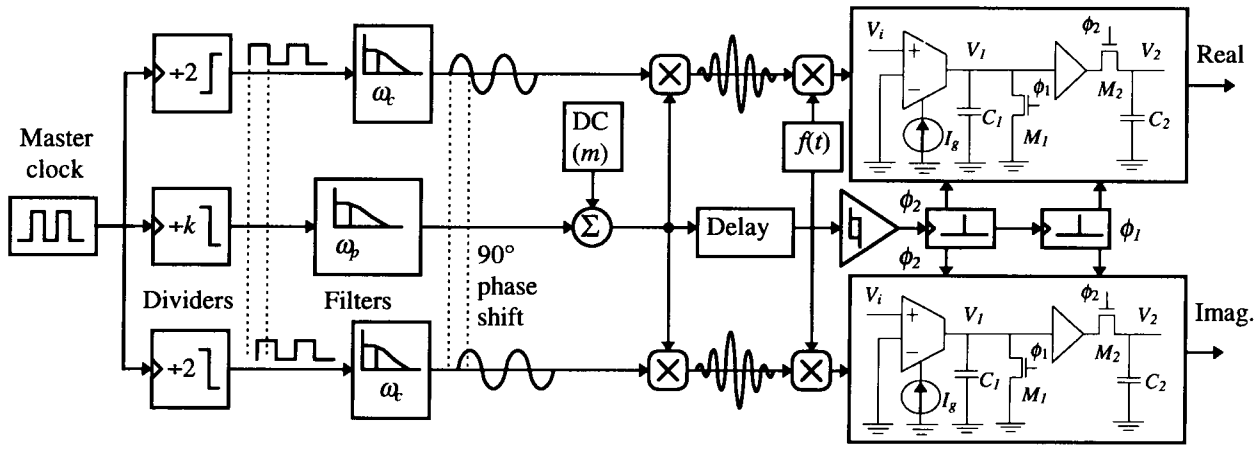

Fig. 3. Hardware implementation approach.

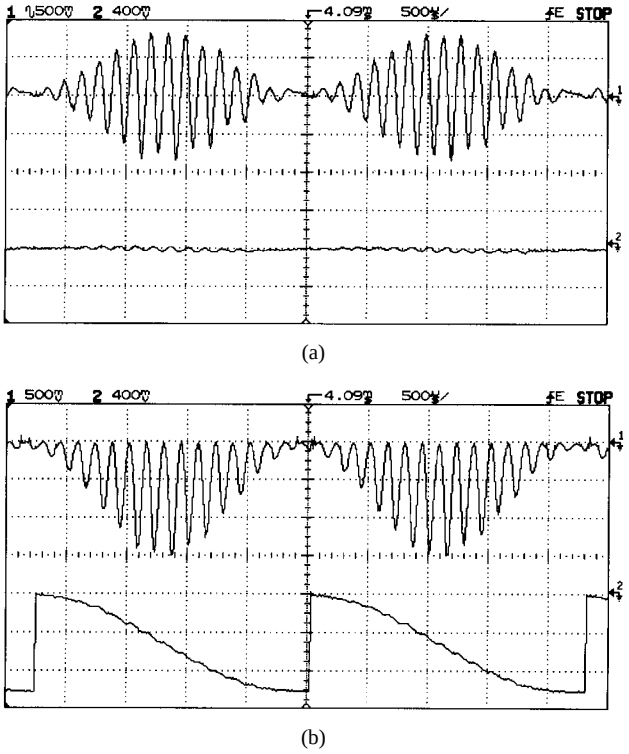

(a)

(b)

Fig. 4. Experimental results of wavelet transform. (a) Result of the multiplication of the real part of the wavelet chain (upper signal) and its integration (lower signal). (b) Same as in (a) for the imaginary part.

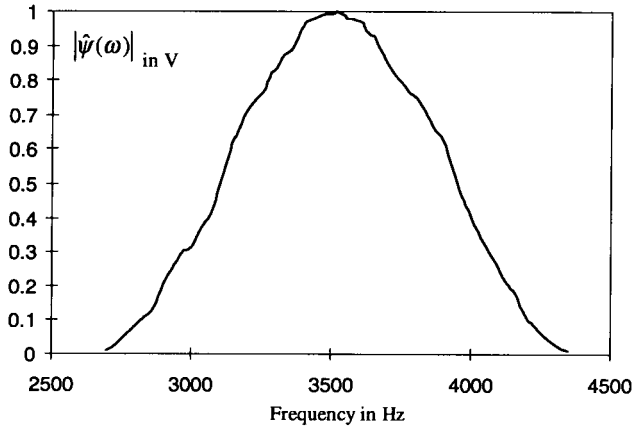

Fig. 5. Frequency response characteristic of the wavelet implemented.

where t_o is the time where the center of the time frequency window is located. Notice that the factor a represents the scaling of the wavelet. If one were analyzing a signal of frequency $\omega_0 = \omega_c$, then a would be set to 1. The integration limits in (2) are given as $-\pi < \omega_p t < \pi$. If the wavelet is scaled for $t \rightarrow t/a$ then the limits become $-a\pi < \omega_p t < a\pi$. Therefore, our integration limits in terms of the window size Δt become $a\Delta t$. In the implementation the limits are evaluated when the cosine function reaches a minimum, e.g., for $m = 1$, the minimum of $v(t)$ is zero and occurs when the argument of the cosine function $\omega_c t/an$ is $-\pi$ or a 2π multiple. The integration process is carried out independently for each wavelet in the chain of wavelets.

At this point we have two individual sinusoidal functions, a cosine and a sine, which are generated and computed separately. The real and imaginary coefficients can have a fast fluctuation due to the phase of the signal. If the input signal is in phase with the real part of the wavelet, the coefficient will be all real (imaginary will be zero). If it is shifted by 90° the coefficient will be imaginary. The coefficients will present a fast fluctuation proportional to the difference in frequency between the input signal and the wavelet. However, if the input signal is constant in some time interval, the magnitude will be constant and the phase will vary. These parts can be obtained by computing the magnitude from (7) as follows:

$$|(W_s f)(a,\, b)| = \sqrt{\mathrm{Re}\,[(W_s f)(a,\, b)]^2 + \mathrm{Im}\,[(W_s f)(a,\, b)]^2}$$
$$\mathrm{Phase}\,[(W_s f)(a,\, b)] = \arctan\left\{\frac{\mathrm{Im}\,[(W_s f)(a,\, b)]}{\mathrm{Re}\,[(W_s f)(a,\, b)]}\right\}. \quad (11)$$

IV. Hardware Implementation

Fig. 3 shows the block diagram for the system implementation. In order to generate orthogonal signals (90° phase shift) with integer multiple frequencies, the signals are generated using a pulse signal (master clock) as the time reference. The master clock (ck_m), is divided using two different flip-flops, one of them triggered by the positive edge and the other by the negative edge (ck_s and ck_c). These two signals are filtered through two equal filters (to have the same phase shift in both signals), passing only the fundamental signal and producing two orthogonal sinusoidals. The envelope can be generated separately or by dividing the master clock and filtering it afterwards, especially when short wavelets are required. The next step is to add a dc component according to the modulation index desired to compose the windowing signal. The modulation index is equal to the magnitude of the sinusoidal divided by the dc component. Then the two sinusoidals are multiplied by the envelope. For our prototype

we used the analog multiplier MC1494. At this point the chain of wavelets similar to the one displayed in Fig. 1 has been generated. Notice that by changing the frequency of the master clock the shape of the wavelet is scaled proportionally. If this happens, the amplitude of the wavelet and the filters' cut off frequency need to be readjusted in order to have a scaled version of the same wavelet.

The wavelet signals are then applied to a convolution section. The wavelets are multiplied by the signal to be analyzed and then integrated. The integrating block was implemented using Operational Transconductance Amplifiers (OTA) [9] and a capacitor C_1. The OTA was chosen because it has the advantage of being electronically programmable, i.e., its transconductance is a function of the current I_g. The integrator is resetted right after the end of each wavelet. Using a pulse ϕ_1 transistor M_1 resets the capacitor C_1. Many applications require interfacing the circuit to a digital system, therefore, a sample and hold circuit is needed. The buffer, transistor M_2, and capacitor C_2 perform this function. The signals that reset the capacitors (ϕ_1 and ϕ_2) are two pulses, their duration must be sufficiently long to fully discharge the capacitors. Observe that the pulse ϕ_2 is used to trigger ϕ_1, i.e., the output is sampled first, and then the integrator is resetted. Pulse ϕ_2 is triggered by a timed signal produced by a comparator circuit. A delayed version of the envelope signal is compared with a threshold voltage producing a square wave. The threshold for the comparator is adjusted to produce a positive flank just before the wavelet ends. This flank triggers an astable multivibrator that produces ϕ_2, i.e., the sampling pulse.

V. Experimental Results

The first test consists of applying different signals to find their wavelet coefficients. The wavelet used for this case-study has an analyzing frequency $\omega_c = 3500$ Hz, modulated by an envelope that has a frequency which is 1/16 of the inner frequency, i.e., $\omega_p = 3500$ Hz/16 $= 218.75$ Hz. Recall that the analyzing frequency must be an integer multiple of the envelope for short wavelets. Fig. 4 shows the results of analyzing a pure sinusoidal signal at the exact same frequency (3500 Hz) of the wavelet but with $+90^\circ$ phase shift with respect to the real part. Fig. 4(a) shows the product of the real part of the wavelet and the input signal, and the result of the integration. Fig. 4(b) shows the same results but for the imaginary part. As expected, the result of integrating the signal in Fig. 4(a) is zero, and the result of integrating Fig. 4(b) is 1.0 V which corresponds to the imaginary part of the wavelet coefficient. Since the real part is zero, the magnitude of this wavelet coefficient is 1.0 V and the phase is $\pi/2$. This voltage is the result of applying a signal at the same frequency as the analysis signal, therefore, it can be used as a normalization parameter. If other signals with different frequencies but the same amplitude are applied, the magnitude of the coefficients will be smaller as Fig. 5 shows. The plot in Fig. 5 was obtained by applying a set of sinusoidal signals with an amplitude of 1 V, covering the frequency range where the magnitude of the coefficient was higher than zero. This is the frequency resolution characteristic of the wavelet employed.

VI. Conclusion

A systematic approach to generate wavelets in time-domain was developed. In particular, we showed the time-domain implementation of Amplitude Modulated Wavelets. Each wavelet transform coefficient is being computed simultaneously as the wavelet is generated and the output is available right after the wavelet is completed. This constitutes a system with minimum delay. The results are suitable for those applications that require fast computation of wavelet coefficients. By using a bank of these circuits a spectral decomposition can be achieved with small computation time.

References

[1] H. H. Szu, C. C. Hsu, P. A. Thaker, and M. E. Zaghloul, "Image wavelet transforms implemented by discrete wavelet chips," *Opt. Eng.*, vol. 33, no. 7, pp. 2310–2325, July 1994.
[2] T. R. Edwards and M. D. Godfrey, "An analog wavelet transform chip," in *ICNN Proc.*, 1993, pp. 1247–1251.
[3] J. Lin, W. Ki, T. Edwards, and S. Shamma, "Analog VLSI implementations of auditory wavelet transforms using switch-capacitor circuits," *IEEE Trans. Circuits Syst. I*, vol. 41, Sept. 1994.
[4] C. K. Chui, *An Introduction to Wavelets.* New York: Academic, 1992.
[5] M. Vetterli and J. Kovacevic, *Wavelets and Subbband Coding.* Englewood Cliffs, NJ: Prentice-Hall, 1995, sec. 2.6.
[6] A. V. Oppenheim and R. W. Schafer, *Discrete-Time Signal Processing.* Englewood Cliffs, NJ: Prentice-Hall, 1989, pp. 447–448.
[7] I. Daubechies, "The wavelet transform, time-frequency localization, and signal analysis," *IEEE Trans. Inform. Theory*, pp. 961–1005, 1990.
[8] P. P. Vaidyanathan, *Multirate Systems and Filter Banks.* Englewood Cliffs, NJ: Prentice-Hall, 1993, ch. 11.
[9] E. Sánchez-Sinencio, R. L. Geiger, and H. Nevarez-Lozano, "Generation of continuous-time two integrator loop OTA filter structures," *IEEE Trans. Circuits Syst.*, vol. 35, Aug. 1988.

Re-examination of Pole Splitting of a Generic Single Stage Amplifier

Wing-Hung Ki, Lawrence Der, and Steve Lam

***Abstract*—Pole splitting on the frequency response of a generic single stage amplifier due to the insertion of a compensation capacitor is re-examined. The Miller's Theorem is discussed in detail and it is shown that the initial dominant pole of an uncompensated amplifier remains dominant after compensation. Input and output impedances are computed to reveal the root loci and bandwidth of these quantities. Simulation results are presented in confirming the analysis**

***Index Terms*—Amplifier design, Frequency compensation.**

I. Introduction

Stability is an important issue in the design of a feedback amplifier. Designers rely heavily on the gain and phase margins in determining the transient performance of an amplifier. Dominant pole compensation with pole splitting is a traditional technique used to obtain adequate phase margin. Fig. 1(a) shows the schematic of a generic single-stage amplifier with a compensation capacitor C_c connected across its input and output ports. Textbook discussions [1]–[4] usually assume that the initial dominant pole is at the input side of the

Manuscript received October 31, 1994. This paper was recommended by Associate Editor S. Mori.

W.-H. Ki is with the Electrical and Electronic Engineering Department, Hong Kong University of Science and Technology, Clear Water Bay, Hong Kong.
L. Der is with Hyundai Electronics America, San Jose, CA 95134 USA.
S. Lam is with Philips Semiconductors, Sunnyvale, CA 94088 USA.

Publisher Item Identifier S 1057-7122(97)00811-8.